

# Exploring Crossing Times and Congestion Patterns at Scramble Intersections in Pedestrian Dynamics Models: A Statistical Analysis

Eduardo V. Stock, Roberto da Silva

*Instituto de Física, Universidade Federal do Rio Grande do Sul, Porto Alegre, Rio Grande do Sul, Brazil*

---

## Abstract

Scramble intersections stand as compelling examples of complex systems, shedding light on the pressing challenge of urban mobility. In this paper, we introduce a model aimed at unraveling the statistical intricacies of pedestrian crossing times and their fluctuations in scenarios commonly encountered in major urban centers. Our findings offer snapshots that faithfully mirror real-world situations. Significantly, our results underscore the importance of two key factors: pedestrian flexibility and population density. These factors play a pivotal role in triggering the transition between mobile and immobile behavior in the steady state, a concept expounded upon within this paper through a straightforward order parameter known as directed mobility.

---

## 1. Introduction

Pedestrian dynamics [1, 2, 3] is a fascinating instance of a complex system with significant implications for urban sustainability and its planning, as highlighted in [4]. The examination of patterns emerging from the counterflowing movement of particles encompasses a broad spectrum of systems, seemingly diverse, including pedestrian dynamics [5, 6, 7, 8, 9] and the motion of charged colloids [10, 11, 12, 13].

Surprisingly, these systems unveil more similarities than one might initially anticipate when it comes to modeling phenomena at both micro and macro scales. Consequently, the emergence of straight lanes and distillation, resulting from the intricate interplay of self-propelled and/or field-directed objects or particles, has ignited a multitude of intriguing questions within the realms of statistical mechanics and stochastic processes in physics. These phenomena are often simulated using Monte Carlo (MC) simulations or expressed through Partial Differential Equations (PDE) [7, 8, 14, 15].

Our research has delved into models considering a two-species counterflow of particles under various circumstances, with and without particle exclusion [7, 8]. More recently, we have explored systems with exclusion, where cell occupancy follows Fermi-Dirac statistics [14, 15]. These systems are particularly intriguing as they reproduce compelling phenomena such as the formation of condensates, metastability, and the coexistence of mobile and clogged states [16], corroborating other numerical findings [17, 18].

Nevertheless, even more complex situations can occur, holding substantial implications for the functioning of cities and urban planning. In this context, the concept of a scramble crossing involving four distinct groups or "species" of people striving to reach their respective objectives, as depicted in Figure 1, becomes relevant. This scenario, as observed in the Ginza district of Tokyo, provides a conspicuous example of human congestion and its impact on urban dynamics.



Figure 1: A typical example of a scramble crossing in urban settings is the bustling Ginza district in Tokyo (image source: Shutterstock).

In this manuscript, building upon our prior modeling work involving two-species counterflowing particles, we present a novel model tailored to capture scenarios exemplified by Figure 1. Leveraging a parameter denoted as  $\alpha$ , which we previously employed in modeling pedestrian dynamics within a nightclub environment [19] to regulate the level of objectivity or orientation of pedestrians toward their destination, in our current context, this parameter pertains to the act of crossing the intersection. Our objective is to investigate the characteristic patterns that emerge at these intersections, analyze the statistical distribution of pedestrian crossing times, and assess the impact of pedestrian density and the degree of orientation or disorientation among pedestrians on these statistical outcomes.

This investigation encompasses several key parameters, including the average duration of the first crossing, its dispersion, as well as higher-order statistics such as skewness and kurtosis for this duration. We closely monitor snapshots of the first crossing to scrutinize the jamming patterns of particles and their natural dispersion within this peculiar scenario. Additionally, we track the temporal evolution of the first crossing times of particles at various time steps.

Beyond this initial crossing analysis, we consider the presence of periodic boundary conditions (PBC) for our particles. Following the initial crossing, the particles continue their movement and

eventually attain a steady state. To observe and analyze this steady state after a certain number of iterations, we employ the concept of *directed mobility*—an intriguing measure that quantifies the extent to which pedestrians move toward their intended destinations, which, in this case, is the opposite side of the intersection during crossings.

After the first crossing time, particles returning to their respective corners act as new individuals entering a street, further contributing to the dynamic behavior of the system.

The structure of our paper is outlined as follows: In the subsequent section, we introduce our model. Section 3 is dedicated to the exploration and analysis of our findings, and, lastly, we present our summaries and draw conclusions in section 4.

## 2. Model

We define our model as a system comprising  $N$  particles, each belonging to one of four distinct types labeled as  $A$ ,  $B$ ,  $C$ , and  $D$ . These particles navigate within an underlying square lattice with dimensions  $L$ . To accurately represent a scramble crossing, we delineate four sidewalk corners by establishing four triangular regions, each centered on one side of our square lattice, as illustrated in Figure 2. Each triangular region possesses a base measuring  $d$  and a height of  $d/2$ . Positioned at each sidewalk corner is a cluster of particles belonging to the same species. These particle types are distinguished solely by their favored direction of movement. Without sacrificing generality, we establish that particles of type  $A$  exhibit a preference for advancing in the  $+x$  direction, particles of type  $B$  tend to move in the  $-y$  direction, particles categorized as type  $C$  gravitate towards the  $-x$  direction, while particles designated as type  $D$  exhibit a tendency to proceed in the  $+y$  direction.

The movement of particles across the lattice occurs cell by cell, governed by a set of stochastic rules inspired by the pioneering work of Montroll and West on clannish random walkers [20], subsequently adapted by da Silva et al. to simulate counterflowing pedestrian dynamics [7]. Our approach shares similarities with other methods, such as the static floor field model found in the literature (see, for instance, [21]). We have tailored this modeling framework to accommodate our specific case involving four distinct species. It's worth noting that our adaptation builds upon the improved modeling techniques proposed in some of our prior contributions [14, 15, 16, 19].

The transition probabilities governing a particle's movement from cell  $(i, j)$  to one of its neighboring cells, say,  $(i + 1, j)$ , are as follows:

$$P_{(i+1,j) \rightarrow (i,j)}^{(l)} = p + \alpha (\Delta \vec{r}_x \cdot \hat{u}), \quad (1)$$

where  $\alpha$  is the coefficient regulating the degree of dynamical bias,  $\Delta \vec{r}_x = \hat{e}_x$  represents the displacement vector, with  $\hat{e}_x$  denoting the unit vector in the  $x$ -direction of our reference frame, and  $\hat{u} = \vec{u}/\|\vec{u}\|$  is the unit vector associated with our static floor field, which guides each particle toward its destination. Specifically,  $\vec{u} = \vec{u}(\vec{r})$ , where  $\vec{r} = i\hat{e}_x + j\hat{e}_y$  denotes the particle's position in Cartesian coordinates. It's important to note that each species within our model perceives its unique static floor field, as their respective preferred directions of movement differ.

As one might anticipate, the transition probabilities for the same particle at position  $(i, j)$  to move to any of its neighboring cells are defined in relation to the displacement vector. Specifically, when the particle hops to  $(i - 1, j)$ , the displacement vector is  $\Delta \vec{r}_x = -\hat{e}_x$ . If it moves to  $(i, j + 1)$ ,

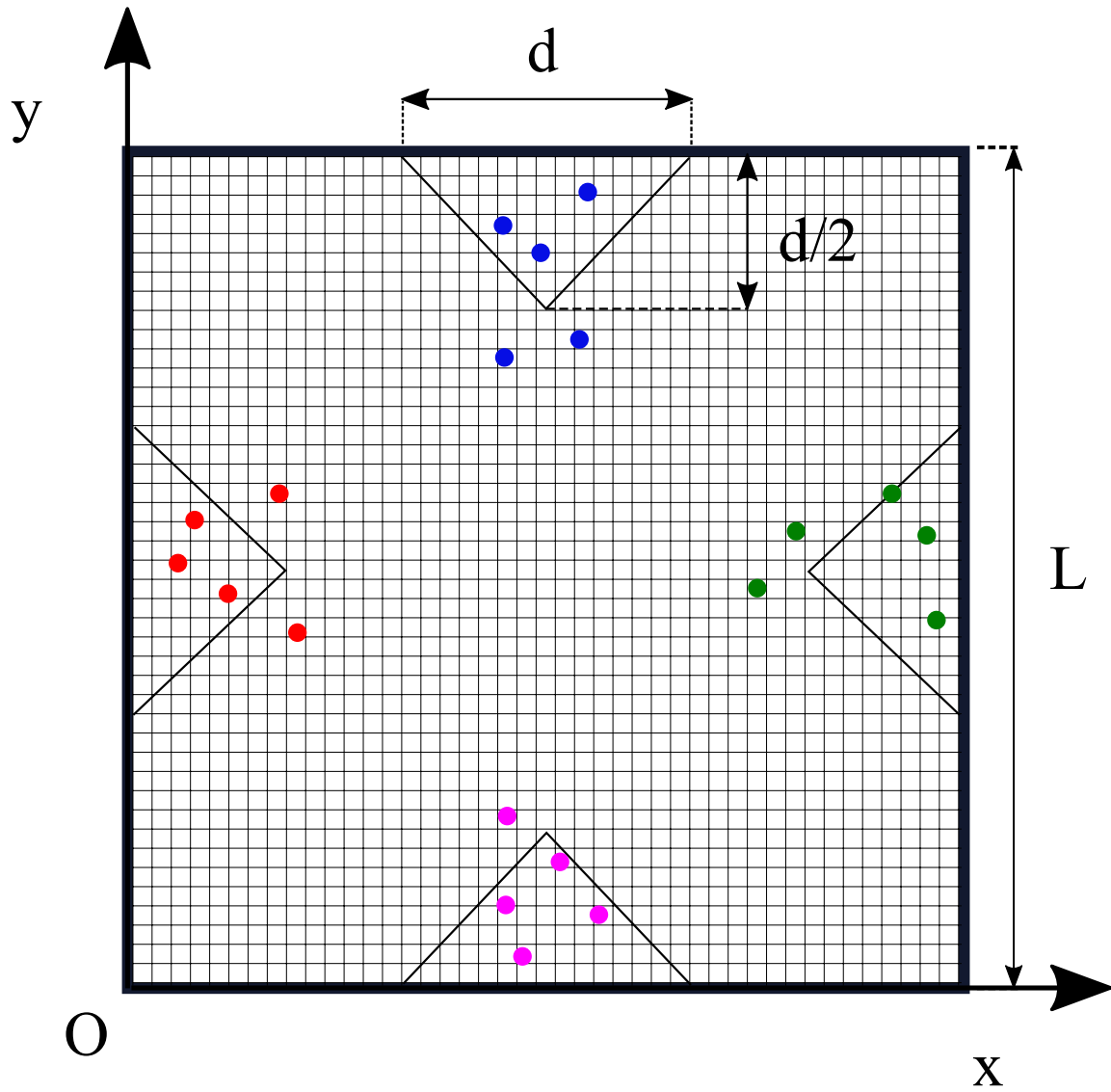


Figure 2: Illustration of a scramble crossing featuring four corners on each side of the lattice. Particles of each type endeavor to traverse the lattice in pursuit of reaching the opposite sidewalk. Specifically, particles of species  $A$  are depicted in red, those of type  $B$  are shown in blue, particles belonging to type  $C$  are represented in green, and particles classified as type  $D$  are denoted in pink.

the displacement vector is  $\Delta\vec{r}_y = \hat{e}_y$ , and if it hops to  $(i, j - 1)$ , the displacement vector becomes  $\Delta\vec{r}_y = -\hat{e}_y$ . To ensure a normalization constraint, the probability that a particle remains in its current cell is expressed as:

$$P_{(i,j) \rightarrow (i,j)}^{(l)} = 1 - \sum_{\langle i,j' \rangle} Pr_{(i,j) \rightarrow (i,j')}^{(l)} = 1 - 4p. \quad (2)$$

To assess the degree of dynamism inherent in the particle's pursuit of reaching the opposite corner, we define *directed mobility* as

$$M_{\vec{u}}^{(l)} \equiv \frac{m_{\vec{u}}^{(l)}}{N}, \quad (3)$$

where  $m_{\vec{u}}^{(l)}$  represents the total number of particles of any kind (all four species are considered) that have moved to a neighboring cell to which their species' static floor field had a vectorial component pointing towards.

We implemented our model through Monte Carlo (MC) simulations, employing an asynchronous update scheme for particle positions. Under this asynchronous updating scheme, during each MC time step, we randomly select  $N$  particles from the total  $N$  particles constituting our system and update their positions sequentially based on the transition probabilities defined earlier.

We will systematically organize our results into two subsections within the upcoming section. Firstly, we strategically placed four groups of particles at the four different corners with carefully chosen initial conditions. Our initial focus lies in analyzing the time required for these particles to make their first crossing of the system.

Secondly, given our implementation of periodic boundary conditions (PBC) for our particles, following this initial crossing, the particles continue to move and ultimately attain a steady state. In this stable configuration, particles return to their respective corners, reminiscent of new individuals entering a street. We delve into this steady state by monitoring the average mobility of the system.

The parameters characterizing the steady-state mobility reveal a transition between a situation where the system remains mobile and one where it becomes congested. This transition is evident in both parameters:  $\alpha$ , which governs the level of objective orientation of pedestrians toward their destination, and  $\rho$ , representing the density of pedestrians, with our results suggesting a relationship between these two parameters in such "crossover" situation.

### 3. Results

We begin our presentation of results by considering an initial condition that mimics a "real-world" scenario. In this setup, all particles are initially positioned at each corner of the four-way scramble crossing, or within the triangular region situated in the middle of each side of our square lattice (as depicted in Fig. 2). In technical terms, this entails that particles of types  $A$ ,  $B$ ,  $C$ , and  $D$  are initially distributed across sites selected at random, subject to the following constraints:

$$x + \frac{L-d}{2} \leq y \leq -x + \frac{L+d}{2}, \quad \text{for } 0 \leq x \leq d/2,$$

$$\begin{aligned}
-y + \frac{3L-d}{2} \leq x \leq y - \frac{L-d}{2}, & \quad \text{for } L-d/2 \leq y \leq L, \\
-x + \frac{3L-d}{2} \leq y \leq x - \frac{L-d}{2}, & \quad \text{for } L-d/2 \leq x \leq L,
\end{aligned}$$

and

$$y - \frac{L-d}{2} \leq x \leq -y + \frac{L+d}{2}, \quad \text{for } 0 \leq y \leq d/2,$$

respectively.

Under the given initial conditions, we embarked on a study of the time required for each agent to complete a single crossing—specifically, reaching either the opposing sidewalk corner or breaching the lattice boundaries (defined as beyond the limits of  $1 \leq x \leq L$  and  $1 \leq y \leq L$ ).

In this preliminary analysis, our primary emphasis is directed towards the concept of “first crossing,” a topic we explore in greater detail in the subsequent subsection. Following this initial investigation, we shift our focus towards scrutinizing the parameters during the steady state, which naturally ensues after several iterations. As mentioned earlier, this steady state simulates a scenario where pedestrians have the green light to cross, and those entering the street assume the roles of new pedestrians.

### 3.1. First time crossing

In Figure 3, we present the first crossing time distribution, taking into account the initial conditions previously specified, across various particle density values. Our simulations encompass a system of dimensions  $L = 128$ , with a corner dimension of  $d = 64$ , and a parameter  $\alpha$  set to 0.249.

Upon examination, it becomes evident that in scenarios characterized by low particle density, the distribution exhibits characteristics resembling a normal distribution, albeit with a slightly negative kurtosis. However, as we transition to higher density scenarios, the distribution undergoes a notable transformation. It begins to exhibit an increase in its root mean square error until reaching a critical point where we observe a more uniform distribution pattern with a broader support. In fact, this transition to higher density scenarios can lead to both shorter and longer first crossing times, a phenomenon attributed to congestion resulting from increased density levels.

The phenomenon of “uniformization” within the distribution of first crossing times becomes clearer when we examine snapshots of the spatial distribution of particles at various time points during the simulation. In Figure 4, we can discern the following trends:

1. Initially, at  $t = 17$  MC steps (depicted in plot (a)), only a limited number of particles from each group disengage from the initial cluster.
2. Over time, around  $t = 622$  MC steps (illustrated in plot (b)), a substantial cluster of particles congregates in the central region of the scramble crossing. This outcome is unsurprising given the high particle density within the system.
3. Furthermore, we observe that a smaller contingent of particles from each species manages to encircle the primary cluster, successfully advancing towards their respective objectives. This seemingly consistent rate at which particles encircle the central cluster plays a crucial role in achieving a uniform distribution of crossing times.

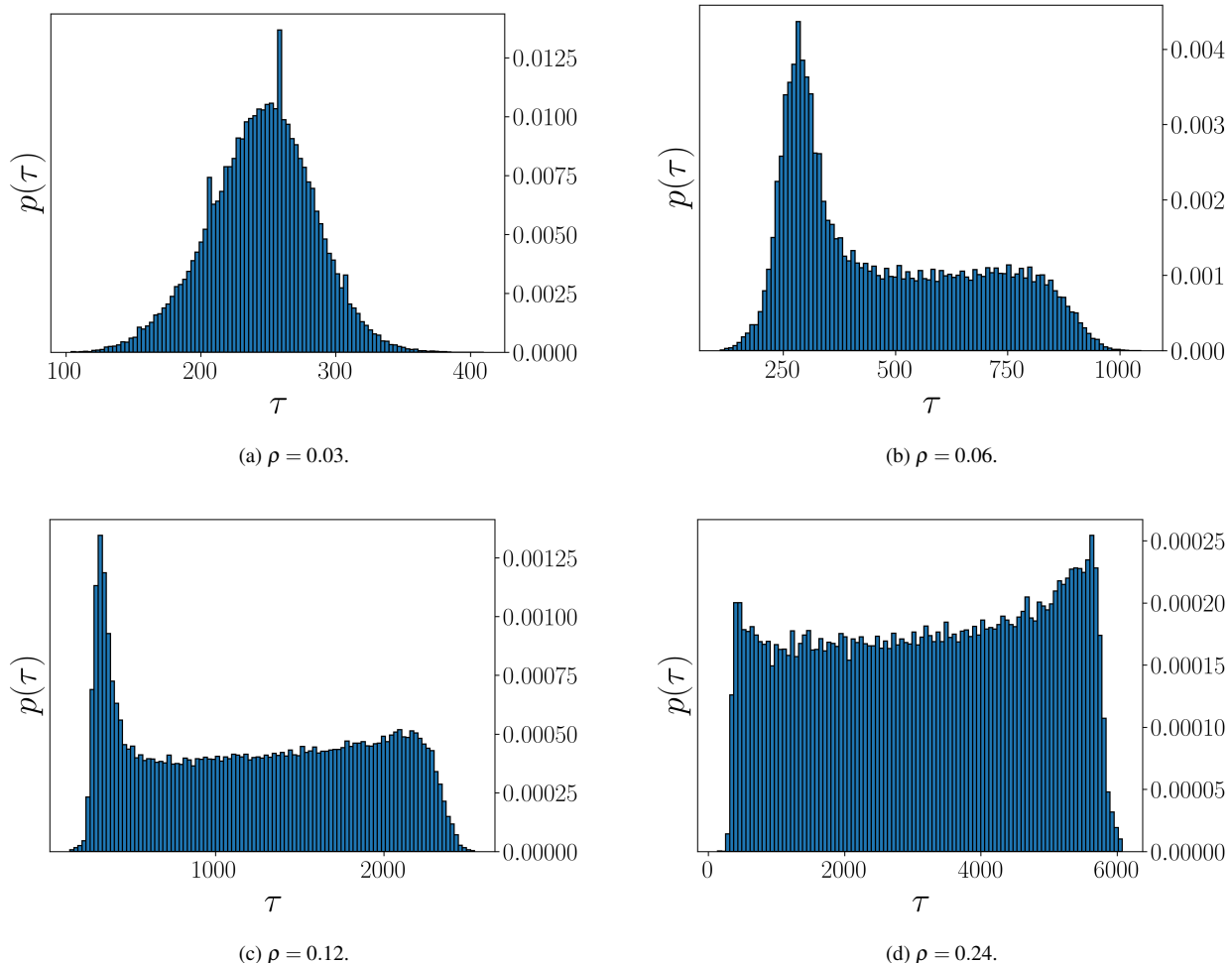


Figure 3: The distribution of first crossing times for various density values within a system characterized by  $L = 128$ ,  $d = 64$ , and  $\alpha = 0.249$ .

4. Ultimately, after a sufficient period has passed, the main cluster disintegrates, leaving only small groups of particles on their individual journeys toward their destinations.

This series of observations sheds light on the dynamic processes at play and how they contribute to the even distribution of crossing times.

Returning to Fig. 3, we can discern distinct patterns in the crossing time distribution, particularly when examining the impact of varying particle densities. In Fig. 3 (a), where the particle density is lower ( $\rho = 0.03$ ), we observe a bell-shaped distribution reminiscent of a normal curve, with an approximate mean value of  $\langle \tau \rangle \approx 250$  MC steps and a standard deviation of  $\sigma_\tau \approx 50$  MC steps.

Moving on to intermediate density values within the range of  $0.03 < \rho < 0.24$ , as depicted in Figs. 3 (b) and 3 (c), we notice a notable shift. While the main peak of the distribution remains consistent, there is now an elongated right tail extending from the peak, resulting in the emergence of a plateau-like feature. This phenomenon aligns with the presence of the central cluster, as

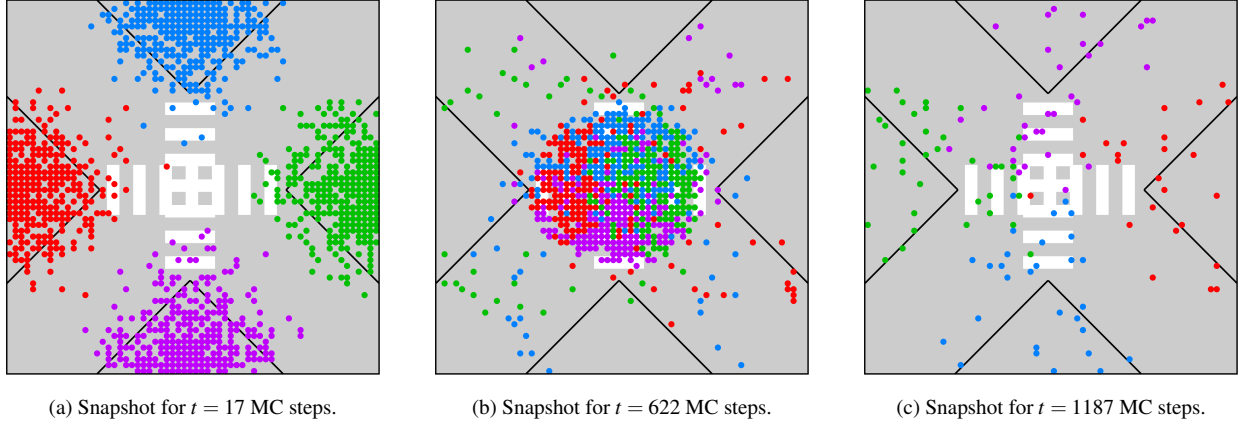


Figure 4: Sequential snapshots depicting the particle distribution at distinct time intervals in a system characterized by  $L = 128$ ,  $d = 64$ ,  $\rho = 0.25$ , and  $\alpha = 0.249$ . In the initial snapshot (plot (a)), select particles detach from the primary group, which remains clustered at the corner. As time advances (plot (b)), a substantial central cluster emerges at the crossing, coexisting with particles employing flanking strategies to reach their destinations. Ultimately, in the final snapshot, the central cluster disperses while some particles continue their journey across the intersection.

observed in Fig. 4 (b). The central cluster fosters a steady influx of particles toward the opposing corner, contributing to the uniform distribution pattern we observe in the crossing times.

Given this behavior, it becomes intriguing to investigate the fluctuations in the first crossing time as a function of  $\rho$  across various  $\alpha$  values, as illustrated in Fig. 5. To do so, we performed  $N_{run}$  simulations (each with a different seed) to obtain a sample size of  $m = 10^5$  crossing times, such that the relation  $N * N_{run} = m$  was maintained.

The average first crossing time is notably influenced by the parameter  $\alpha$ . A minor increase in this orientation parameter leads to a decrease in the average time, with a lesser dependence on  $\rho$ , as evident from our observations. In contrast, the dispersion, denoted as  $\sigma_\tau$  and calculated as the difference between the second moment  $\langle \tau^2 \rangle$  and the square of the first moment  $\langle \tau \rangle^2$ , exhibits a strong dependence on particle density for  $\alpha > 0$ . This finding aligns with the observations presented in Fig. 3. Furthermore, other significant statistical measures, including higher moments of the first-time crossing distribution, such as skewness:

$$skew = \left\langle \left( \frac{\tau - \langle \tau \rangle}{\sigma_\tau} \right)^3 \right\rangle, \quad (4)$$

and the heaviness of the distribution tail which is quantified by the excess kurtosis, obtained by subtracting 3 from the fourth central moment

$$kurt = \left\langle \left( \frac{\tau - \langle \tau \rangle}{\sigma_\tau} \right)^4 \right\rangle - 3, \quad (5)$$

also present a substantial dependency on density for  $\alpha > 0$ . The key takeaway is that, regardless of the pedestrians' orientation levels, if it is only positive, we consistently observe a significant influence on the shape of the first crossing distribution.



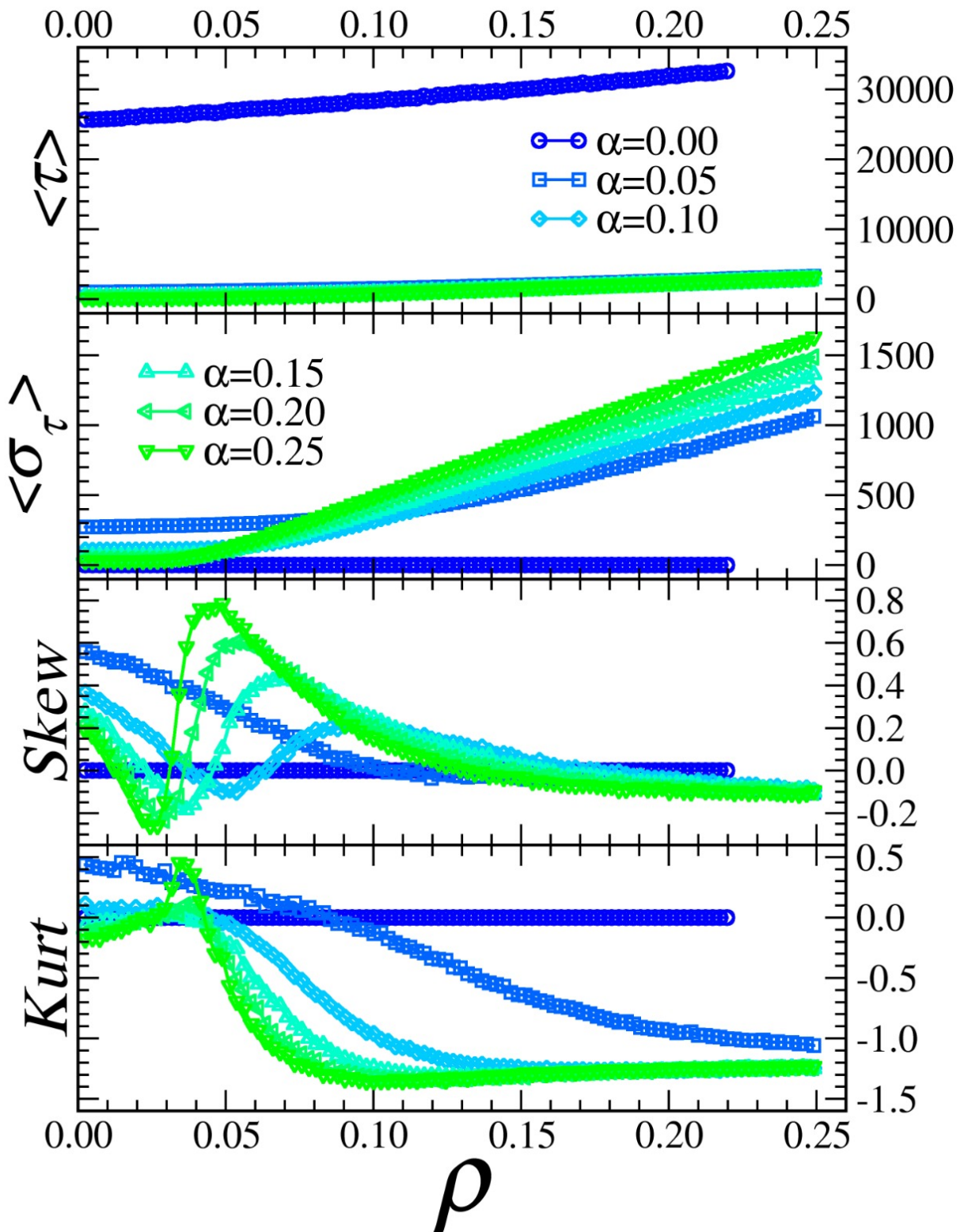
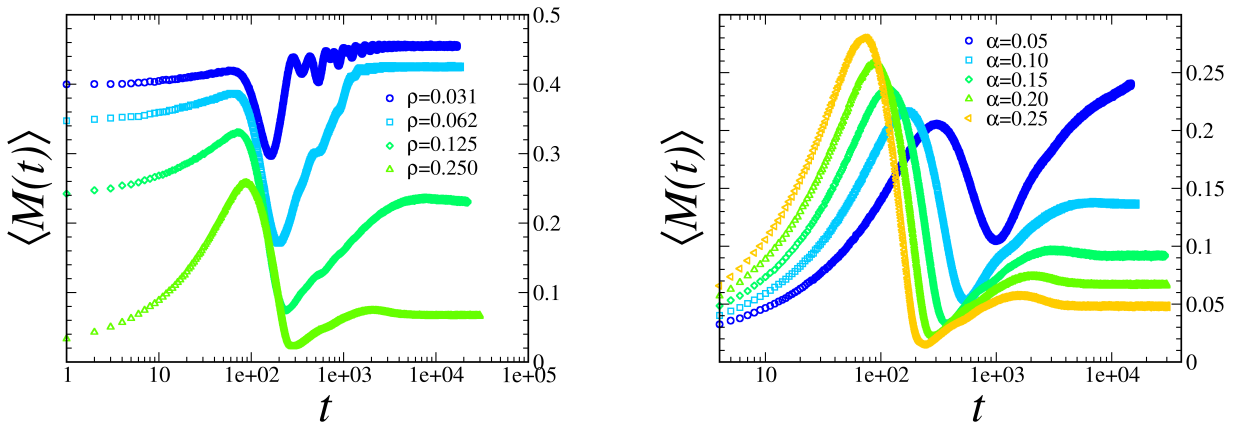


Figure 5: Analyzing crossing time statistics across various  $\alpha$  values as a function of the density of pedestrian  $\rho$ .

Now, we will investigate the dynamics under periodic boundary conditions to monitor mobility (as defined in Eq. 3) in the steady state as a function of  $\alpha$  and  $\rho$ .

### 3.2. Periodic boundary conditions

We now turn our attention to analyzing the dynamics of intersection crossing, taking into account periodic boundary conditions (PBC). Initially, we investigate the time-dependent behavior of average mobility ( $\langle M \rangle$ ) obtained from  $N_{run} = 100$  different time series) across various densities, as depicted in Fig. 6 (a). In this analysis, we maintain  $\alpha$  at a fixed value of 0.2. Notably, we observe mobility undergoing fluctuations, both increasing and decreasing, before eventually reaching a steady state, the characteristics of which are density-dependent.



(a) Time series of the average mobility for different densities, with a fixed value of  $\alpha = 0.2$

(b) Time series of the average mobility for different values of  $\alpha$ , while keeping  $\rho$  fixed at 0.25.

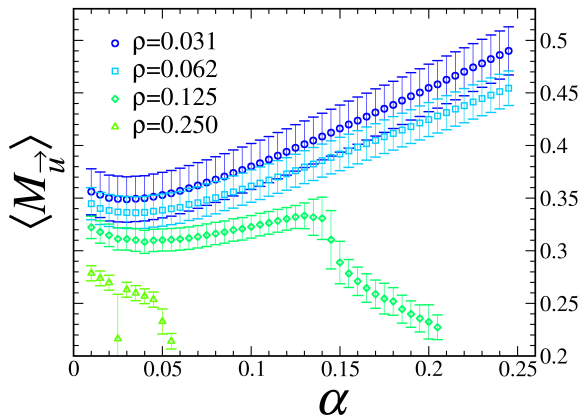
Figure 6: Time series illustrating the averaged directed mobility across  $N_{run} = 100$  samples.

The substantial reduction in mobility corresponds to the initial competition among particles, as they contend with counterflow and congestion. As depicted in Fig. 6 (b), the average mobility varies across different values of  $\alpha$ . Notably, it is crucial to observe that for lower orientation levels (lower  $\alpha$  values), the attainment of a steady state is anticipated to require a significantly longer time, in line with our intuitive expectations.

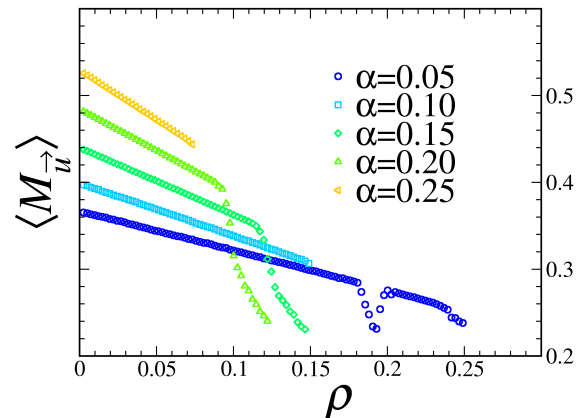
We now delve into an analysis of the average directed mobility in the steady state, examining their dependency on the parameters  $\alpha$  and  $\rho$ . Specifically, we explore the impact of varying  $\rho$  values in the first part and different  $\alpha$  values in the second. These findings are presented in Figs. 7 (a) and 7 (b), respectively, where we performed  $N_{run}$  simulations observing the relation  $N * N_{run} = m$  for a sample size of  $m = 10^5$ .

In Fig. 7 (a), we observe that by adjusting the density ( $\rho$ ), we can anticipate a transition between a mobile and an immobile phase of particles, characterized by a critical value  $\alpha_C(\rho)$ . This transition highlights that high orientation, which represents pedestrians with lower flexibility, tends to lead to congestion scenarios.

Similarly, in 7 (b), we identify a critical density  $\rho_C(\alpha)$  that determines the transition between mobile and immobile phases as  $\alpha$  varies.



(a) Steady-state average mobility as a function of  $\alpha$  across various density values.



(b) Steady-state average mobility as a function of  $\rho$  across different values of  $\alpha$

Figure 7: We note that higher values of  $\alpha$  enhance mobility for lower densities ( $\rho < 0.125$ ). However, beyond a certain threshold, specifically within the range of  $0.062 < \rho < 0.125$ , we observe a decrease in mobility when particles exhibit strong oriented movement (no flexible pedestrians)

#### 4. Summaries, conclusions, and discussions

We have gathered valuable insights into pedestrian crossing times within the intricate settings of typical urban corners in large cities. Our results reveal instances of congestion that arise not only during the initial competitive phase among pedestrians but also persist in the steady state. This congestion is contingent on the interplay between two crucial factors: the orientation level  $\alpha$  and the pedestrian density  $\rho$ . Our findings underscore that the flexibility and concentration of pedestrians play pivotal roles in facilitating smooth crossings at complex intersections in bustling urban centers.

Furthermore, we have observed a noteworthy transition between mobile and immobile phases during the steady state, a transition that hinges on the values of both  $\alpha$  and  $\rho$ . It is worth emphasizing that the concept of direct mobility has proven to be an invaluable parameter for analyzing both transient and steady-state dynamics in pedestrian behavior within such complex environments.

#### References

- [1] D. Helbing and P. Molnar, Phys. Rev. E 51, 4282 (1995)
- [2] W. Daamen, S. Hoogendoorn, M. Campanella, D. Versluis Interaction Behavior Between Individual Pedestrians. In: Weidmann, U., Kirsch, U., Schreckenberg, M. (eds) Pedestrian and Evacuation Dynamics 2012. Springer, Cham. [https://doi.org/10.1007/978-3-319-02447-9\\_107](https://doi.org/10.1007/978-3-319-02447-9_107)
- [3] Z. Fu, Y. Feng, X. Xiong, Y. Yang, L. Luo, J. Li, Physica A **625**, 128983 (2023)
- [4] J. L. Baeza, J. Carpio-Pinedo, J. Sievert 1, A. Landwehr, P. Preuner, K. Borgmann, M. Avakumović, A. Weissbach, J. Bruns-Berentelg, J. R. Noennig, Sustainability **13**, 9268 (2021)
- [5] Y. Tajima, K. Takimoto, and T. Nagatani, Physica A 313, 709 (2002)
- [6] H. Ohta, EPL, **99**, 40006 (2012)
- [7] R. da Silva, A. Hentz, A. Alves, Physica A **437**, 139 (2015)
- [8] E. V. Stock, R. da Silva, H. A. Fernandes, Phys. Rev. E **96**, 012155 (2017)

- [9] Q.-Y. Hao a, J.-L. Qian , C.-Y. Wu , N. Guo, *Physica A* **567**, 125688 (2021)
- [10] J. Dzubiella, G. P. Hoffmann, and H. Lowen *Phys. Rev. E* **65**, 021402 (2002)
- [11] M. Rex and H. Lowen *Phys. Rev. E* **75**, 051402 (2007)
- [12] T. Vissers, A. van Blaaderen, A. Imhof. *Phys. Rev. Lett.* **106**, 228303 (2011), T. Vissers, A. Wysocki, M. Rex, H. Lowen, C. P. Royall, A. Imhof, and A. van Blaaderen, *Soft Matter* **7**, 2352 (2011)
- [13] I. Buttinoni, J. Bialke, F. Kummel, H. Lowen, C. Bechinger, and T. Speck, *Phys. Rev. Lett.* **110**, 238301 (2013)
- [14] R. da Silva and E. V. Stock, *Phys. Rev. E* **99**, 042148 (2019)
- [15] E. V. Stock, R. da Silva, C. R. da Cunha, *J. Stat. Mech.* 083208 (2019)
- [16] E. V. Stock, R. da Silva, *Phys. Rev. E* **102**, 022139 (2020)
- [17] C. Appert, L. Santen, *Phys. Rev. Lett.* **86**, 2498 (2001)
- [18] R. Barlovic, L. Santen, A. Schadschneider, M. Schreckenberg, *Eur. Phys. J. B* **5**, 793 (1998)
- [19] E. V. Stock, R. da Silva, *Chaos, Solitons & Fractals*, **168**, 113117 (2023)
- [20] E. W. Montroll and B. J. West. Chapter 2: On an enriched collection of stochastic processes. *Fluctuation phenomena* Ed. by E. W. Montroll, J. Lebowitz (1979)
- [21] S. Nowak, A. Schadschneider, *Phys. Rev. E* **85**, 066128 (2012)

### **CRedit authorship contribution statement**

All authors conceived and designed the analysis, performed formal analysis, wrote the paper, elaborated the algorithms, analysed the results, and reviewed the manuscript.

### **Declaration of competing interest**

The authors declare that they have no known competing financial interests or personal relationships that could have appeared to influence the work reported in this paper

### **Funding**

R. da Silva would like to thank CNPq for financial support under grant number 304575/2022-4. E. V. Stock also thanks CNPq for financial support under grant numbers 152715/2022-3.